Paper No. 35

THE ABLATION PERFORMANCE OF FOAMS IN A LOW HEAT FLUX

D. H. Smith and D. R. Hender, *McDonnell Douglas Astronautics Company, Huntington Beach, California*

ABSTRACT

Tests of ablation performance of low-density, polyurethane-based foams have been conducted in a low-heat-flux plasma-arc environment. It is shown that fire-retardant chemicals included in the foam have a significant effect in reducing surface recession, and that these materials are attractive candidates for ablative cryogenic insulation systems.

INTRODUCTION

A wide range of future space missions will employ large cryogenic tanks, either as payloads or as launch stages, which will require an insulation system that must not only minimize ground-hold boiloff and propellant quality degradation but also resist the surface erosion caused by aerodynamic heating. Conventional procedures usually dictate the screening of numerous proven ablators for their ability to adhere to cryogenic surfaces. In this study, however, materials with proven cryogenic insulation capabilities were modified to enhance their ablative performance.

The materials investigated are shown in Table 1 and included the Saturn S-II polyurethane spray-foam material, BX-250; two pour foams, BX-251 and CPR-421; a one dimensionally reinforced foam (Z-direction fibers), BX-251-1D; and the MDAC-W "filled" foams, XF-2 through XF-7, which are essentially different-density versions of a polyurethane pour foam to which various amounts of fire-retardant chemicals have been added.

ABLATION TESTS

The tests were conducted at the McDonnell Douglas Research Laboratories (MDRL) Plasma Arc Tunnel (PAT) Facility (Figure 1) in St. Louis, Mo. The aerodynamic heating environments expected during ascent flight encompass heating rates ranging from near zero to 6 Btu/ft^2 sec. Since this heating level could not be attained in the conventional stagnation or splash mode of material exposure, it was necessary to consider

Table 1 Materials Tested

Foam	Density	Component Weight Percent			
		Polyurethane Foam	$NH_4HBO_4O_7 \cdot 3H_2O$	$(NH_4)_2HPO_4$	Other
BX-250	2.6	100			
BX-251	1.7	100			
BX-251-1D	3.0	80			20-Nylon Thread
XF-1	1.9	100			
XF-2	3.3	72	14	14	
XF-3	4.6	72	14	14	
XF-4	8.0	72	14	14	
XF-5	3.5	84	8	8	
XF-6	4.5	84	8	8	
XF-7	3.5	84		16	
CPR-421	2.0	Proprietary Foam (CPR Div., Upjohn Co.) Polyurethane Base			

WD 2196

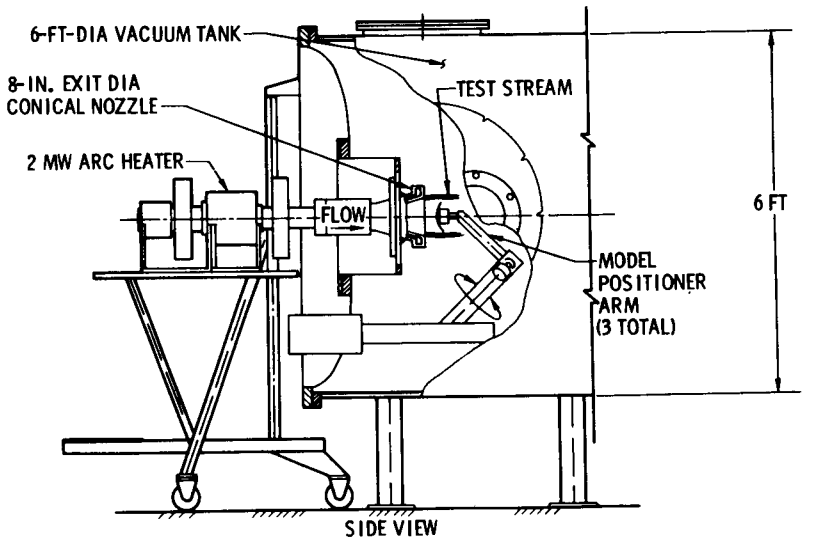

Fig. 1—Schematic of McDonnell Douglas plasma arc tunnel

a sample orientation parallel to the plasma stream, coupled with the use of secondary air injection downstream of the plasma arc to reduce the stream enthalpy. The nominal test environments achieved in this way ranged from 2 to 10 Btu/ft^{2}sec.

A special water-cooled holder was designed by PAT personnel to enable two 2-in. square samples of material to be tested simultaneously, one on each side of the holder. The edges were left exposed so that motion pictures could be taken of the samples during the test to obtain recession data. Figure 2 shows the holder with a calibration plate in place. The holder's leading edge was positioned vertically 2 in. downstream of the nozzle exit plane.

WD 2196

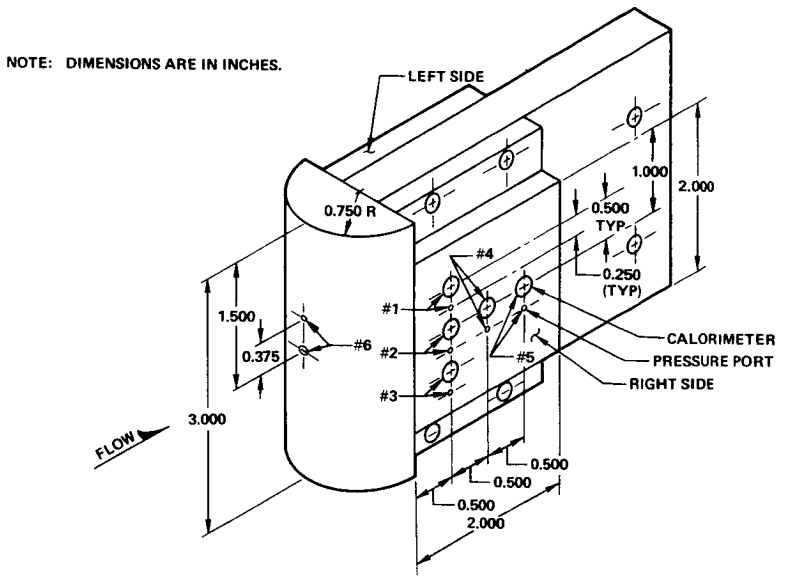

Fig. 2—Model holder with calibration plate installed

For the first test series, heating rate and pressure were measured with this instrumentation (Figure 2). The right-side calibration plate (containing pressure taps and heat flux sensors) was maintained flush during each exposure. The left-side plate (containing only heat flux sensors) was changed from flush to recessed depths of 1/16 in. and 1/8 in. Table 2 summarizes a typical calibration series. The heating rate to the calibration plate was reduced when recessed 1/16 in. but no further reduction was noted at a depth of 1/8 in.--somewhat inconsistent with the aft-facing step results of Nestler et al (Reference 1).

Table 2 Pressure and Heating Rate Distribution as a Function of Surface Position*

	Pressure (torr)					Heating Rate (Btu/ft^2-sec)				
	1	2	3	4	5	1	2	3	4	5
Right Calorimeter (Flush)	0.52	0.49	--	0.43	0.40	2.2	2.2		1.5	1.6
Left Calorimeter (Flush)	--	--	--	--	--	2.1	1.9		1.4	1.7
Stagnation Line			9.44					23.3		
Right Calorimeter (Flush)	0.54	0.53	--	0.46	0.43	2.1	2.0	2.1	1.4	-
Left Calorimeter (1/16 in. recessed)	--	--	--	--	--	1.8	1.6	1.6	1.0	1.4
Stagnation Line			9.33					24.0		
Right Calorimeter (Flush)	0.53	0.53	--	0.44	0.44	2.1	2.1	2.1	1.4	1.6
Left Calorimeter (1/8 in. recessed)	--	--	--	--	--	1.8	1.5	1.5	1.1	1.4
Stagnation Line			9.35					24.9		

*See Fig. 1 for location of sensors 1 through 5.

During later tests, a calibration plate was made up with seven copper-slug calorimeters in the direction of the flow to provide more definition of the streamwise heating gradients as well as the effect of smaller recessed increments. Unfortunately, the results were inconclusive since the changes in arc conditions from run to run and deviations in the measurement of calorimeter slopes overshadowed any other trends.

Instrumentation of the material samples consisted of three chromel-alumel thermocouples per sample. Two were located at the sample-backup structure interface on the centerline, and one was at the geometric center of the ablative material (Figure 3).

Supplemental surface-temperature information was obtained from a TD-17 optical pyrometer, sighted on the right-side sample surface 1/2 in. downstream of the leading edge and on the centerline. The pyrometer was sighted through a calcium fluoride window with 92-percent transmission in the 1.7-to 2.6-micron range, with the pyrometer emittance set to 1.0.

Table 3 summarizes the test foams and their performance. Since most of the materials ablated smoothly and uniformly, recession- and heating-rate data are only given for the model's trailing edge, farthest from the influence of the step formed

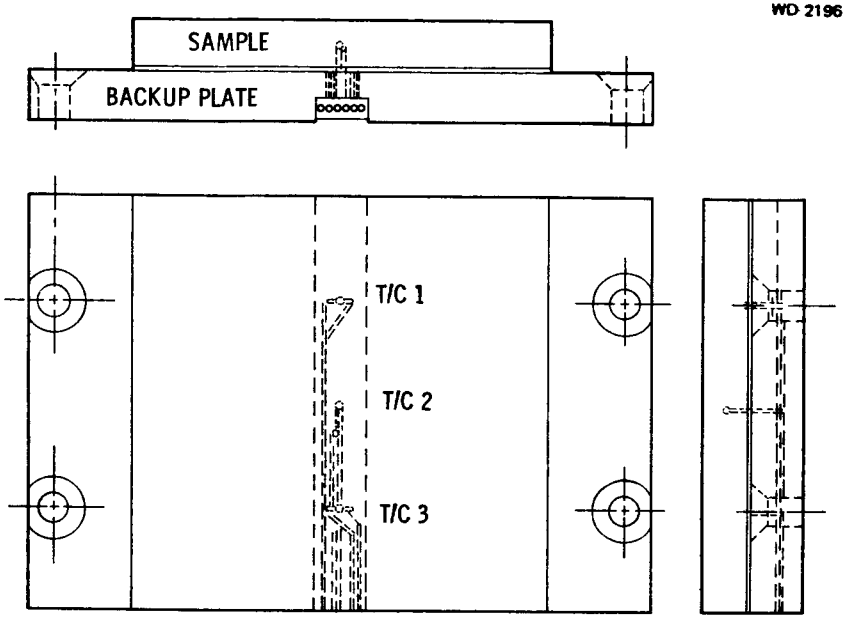

Fig. 3—Ablation sample and backup plate

when the model's front edge recedes below the holder's surface. Back-face temperature rise reflects the response of the aft-most thermocouple (No. 3). All data are averaged for both models on each side of the holder.

The basic polyurethane foams--BX-250, BX-251, XF-1, and CPR-421--showed a moderate resistance to low-level heating rates, and performed better than expected. In applications where the surface radiation equilibrium temperature reaches 600 to 700°F for short periods of time, the resultant ablation can be incorporated in the overall cryogenic insulation thickness requirements. For higher heating-rate environments, however, the performance deteriorates rapidly, and it would be advantageous to consider other material formulations. The XF series of ablative foams (XF-2 through XF-7) show a significant improvement in ablation resistance over the basic polyurethane foams. Where aerodynamic heating rates exceed acceptable limits for the basic foams, these materials offer an ideal alternative, combining good cryogenic insulation qualities with moderate ablative performance.

ANALYTICAL MODELING

The ablation of a number of these materials was calculated using the CHAMP charring ablator program (Reference 2)

Table 3 Ablation Test Program Summary

Foam	Heat Rate (Btu/ft²sec)	Enthalpy† (Btu/lbm)	Duration (sec)	Surface Recession (in.)	Backface Temperature Rise (°F)	Peak Pyrometer Reading (°F)	Weight Loss (%)
BX-250	1.50	2,150	120	0.11	118	660	81
BX-250	1.43*	2,050	140	0.146	100		
BX-250	2.32	3,050	60	0.168	105		
BX-250	3.26	3,300	16	0.172	150		
BX-251	1.50	2,000	65	0.12	95	545	69
BX-251-1D	1.60	2,050	280	0.05**	412	660	
CPR-421	1.65	2,340	342	0.098***	160	705	
XF-1	1.85	2,150	69	0.10	97	612	81
XF-2	1.60	2,100	425	0.07	130	585	
XF-3	1.70	2,050	425	0.06	160	600	72
XF-3	3.55	3,290	200	0.026	120		
XF-3	6.35	4,670	185	0.062	480		
XF-4	1.80	2,050	425	0.02	175	585	35
XF-5	1.80	2,650	425	0.066	610		
XF-5	3.60	3,590	44	0.084			
XF-6	1.60	2,350	425	0.028	80	592	
XF-6	4.45	3,620	168	0.090	103	950	
XF-6	6.35	4,525	180	0.119	450		
XF-7	1.70	2,340	429	0.144	170	645	

*Higher aero shear
**Material receded between threads
***Large areas in center of specimen totally eroded
†Bulk enthalpy. Recovery enthalpy is approximately 85% of this value.

parametrically to determine steady-state ablation rates caused by diffusion-controlled oxidation modified by blowing, with equilibrium boundary layer chemistry plus rate-controlled pyrolysis and surface oxidation. An empirical chemical formula, $C_wH_xO_yN_z$, was determined for the virgin and charred forms of each material studied, based on data from thermo-gravimetric analysis (TGA) and knowledge of the chemical constituents. It was assumed that all foams had cells filled with Freon 11 ($CFC\ell_3$) foaming agent, and the empirical formula was modified to account for this, assuming that the halogen molecules could be treated as effectively as a mixture of oxygen and nitrogen:

$$C\ell_3\,F \sim O_2 + z'N$$

where z' was determined so that the equation balances in mass.

The borate and phosphate salts indicated for many of the foams listed in Table 1 are fire-retardant chemicals added to the foams to improve their ablation performance. For foams containing these salts, the empirical formula was further modified to account for the products of the salts' thermal decomposition. It was assumed that the final reduction products would be B_2O_3 that would remain in the material as a solid, and P_4O_6 that would be driven off as a gas. The fraction of residue seen in the TGA data on these salts agrees well with those calculated under these assumptions.

Five types of foams were modeled using these techniques: BX-250, BX-251, XF-3, XF-6, and a polyurethane foam with 7-percent KBF_4, described in Reference 3. Good agreement was obtained with the data of Reference 3, and with the BX-250 and BX-251 data for heat fluxes below 2 Btu/ft^{2}sec. However, where the heating exceeded this, the ablation performance of BX-250 and BX-251 rapidly diverged from the thermochemical predictions. Figure 4 presents a summary of the nondimensionalized ablation rates scaled from side-aspect movies of the BX-250 and BX-251 tests along with the thermochemical curve.

WD 2196

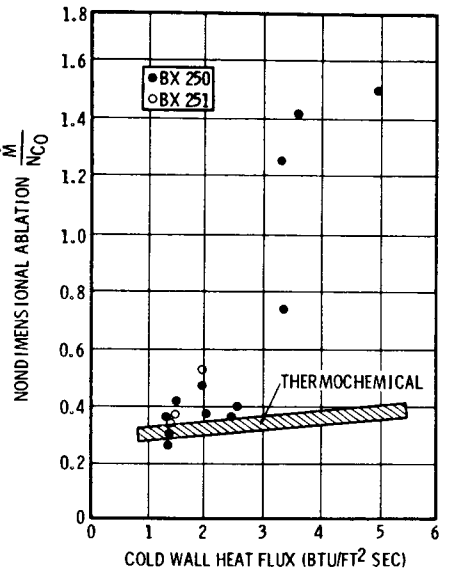

Fig. 4—BX-250 and BX-251 ablation summary

In this series of analyses, it was found that, analytically, oxidation is bistable at the temperatures and pressures of these tests. Equilibrium chemistry predicts that either of the following reactions is possible:

$$2H_2 + 2O_2 + C \rightarrow 2H_2O + CO_2$$

$$2H_2 + 2O_2 + 4C \rightarrow 2H_2 + 4CO$$

The SCREEN reaction-rate chemistry program (Reference 4) predicts that the second reaction would dominate in a mixture of molecular hydrogen, oxygen, nitrogen, and atomic carbon; however, it also predicts that a mixture of the products of the first reaction would revert extremely slowly

toward the products of the second. Obviously, to obtain realistic ablation rate predictions it is essential to select the proper reaction, since ablation rates are much higher with the second reaction because most of the carbon must come from the removal of surface material. Figure 5 shows the predicted non-dimensional ablation rates for both oxidation modes. The predictions shown in Figure 4, and the correlation with the results of Reference 3, represent recession predicted with the second oxidation reaction.

WD 2196

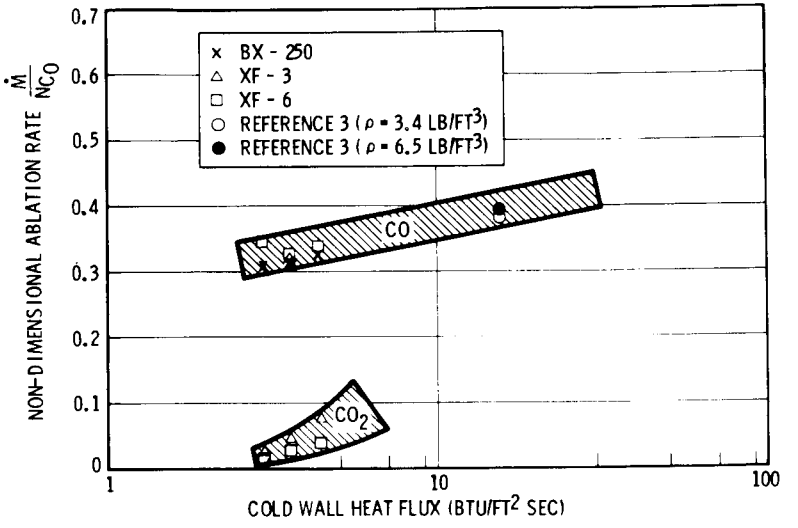

Fig. 5—Thermochemical steady-state ablation predictions

Ablation of foams with salts generally differs considerably from that of BX-250 and BX-251. Initially, their recession rate seems to be about the same as for the plain foams, but, it drops much lower after 15 to 20 sec. Post-test inspection of the samples shows that the foams with added salts form a soft porous char with a delicate crusty surface, while the plain foams do not. It is not clear why this char formation affects ablation rates; however, it was noted that the recession rates predicted using the first oxidation reaction match quite well those seen in the latter phase of the tests, as shown in Figure 6. Apparently, as the carbon in the char is removed by oxidation, the salt residue remains on the surface and changes the character of the surface chemical reactions after ablation reaches some critical depth. It is felt that the significant additive causing this is boron, both because a pair of samples containing only the phosphate (XF-7) was tested and performed quite poorly, and because the foams

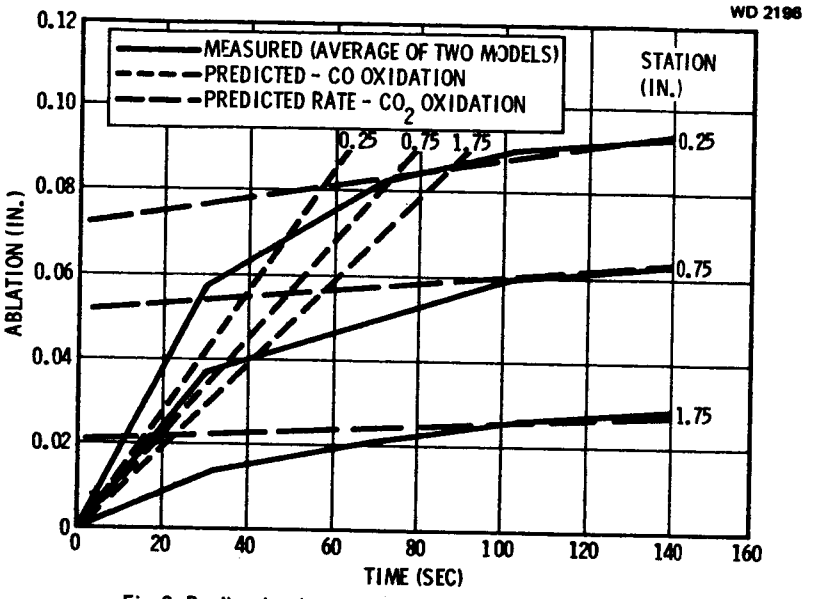

Fig. 6—Predicted and measured ablation for XF-6 (run 3629)

of Reference 3 also contain a boron compound. This critical ablation depth can be fairly well correlated by an equation of the form of the Arrhenius equation, as shown in Figure 7, using the radiation equilibrium surface temperature and the concentration of boron in the material:

$$\Delta S_{critical} = \frac{1}{\rho_{boron}} A e^{-\frac{B}{T_e}}$$

CONCLUSIONS

Foams appear to be very attractive ablation materials for low-heat-flux applications. Standard polyurethane foams tested have good ablation resistance for heat fluxes below 2 Btu/ft^{2}sec, while modified foams have demonstrated ablation resistance many times better. Figure 8 shows the regimes of applicability of both types. With their low density and conductivity, and ablation rates as low or lower than most denser ablators, foams are attractive candidates for many ablative protection roles, especially where cryogenic insulation is required.

ACKNOWLEDGMENT

This work was sponsored by the McDonnell Douglas Astronautics Company and performed under Independent Research and Development.

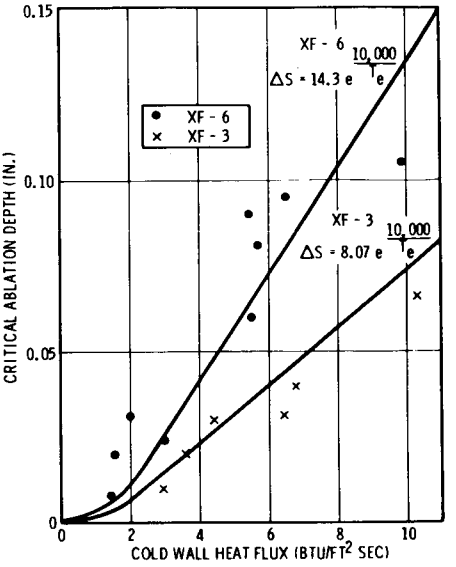

Fig. 7—Critical ablation depth for modified foams

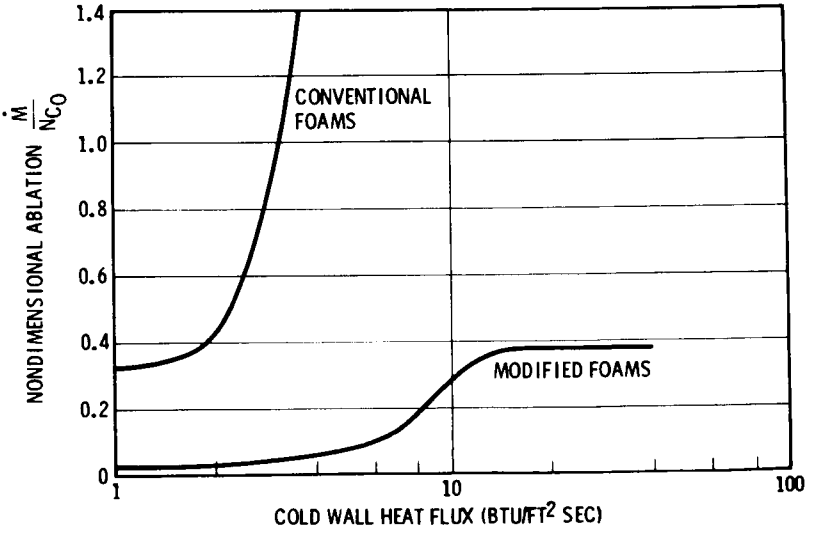

Fig. 8—Foams' ablation regimes

SYMBOLS

A	Empirical coefficient	$\frac{\text{in.-lb}}{\text{ft}^3}$
B	Empirical coefficient	°R
$\dot{M}$	Mass loss rate	$\frac{\text{lb}}{\text{ft}^2\ \text{sec}}$
N_{C_O}	Non-blowing enthalpy heat transfer coefficient	$\frac{\text{lb}}{\text{ft}^2\ \text{sec}}$
T_e	Radiation equilibrium temperature for a black surface	°R
ρ	Material density	$\frac{\text{lb}}{\text{ft}^3}$

522-137 O - 73 - 32

REFERENCES

1. Nestler, D. E., et al. Heat Transfer to Steps and Cavities in Hypersonic Turbulent Flow. AIAA Paper No. 68-673, June 1968.

2. Arne, C. L. Charring Ablator Multiphase Processes Computer Program. Douglas Report SM-49310, July 1966.

3. Pope, R. B., S. R. Riccitielo, and H. E. Goldstein. Ablative Thermal Protection at Low Heating Rates. Materials Journal, SAMPE Quarterly, Vol. I, No. 1.

4. Frey, H. M. and G. R. Nickerson. A Computer Program for the Screening of Chemically Reacting Gas Mixtures. Dynamic Science Report No. TR-141-1-CS, February 1970.